BSGF - Earth Sciences Bulletin 2021, 192, 39
© N. Tribovillard, Published by EDP Sciences 2021
https://doi.org/10.1051/bsgf/2021034

BSGF
Earth Sciences Bulletin
Available online at:
www.bsgf.fr

Open Access

Conjugated enrichments in arsenic and antimony in marine deposits used as paleoenvironmental proxies: preliminary results

Nicolas Tribovillard*

Univ-Lille, CNRS, Univ Littoral Côte d'Opale, UMR 8187 LOG, Laboratoire d'Océanologie & Géosciences, F-59000 Lille, France

Received: 16 November 2020 / Accepted: 1 September 2021 / Publishing online: 22 September 2021

Abstract – Two redox-sensitive metalloids, arsenic (As) and antimony (Sb), are examined here to determine what can be their help in the deciphering of past depositional conditions. The enrichment factors of the two elements are compared for a set of geological formations and marine deposits covering a relatively wide range of paleoenvironmental settings, from oxic to euxinic conditions. This work confirms that As and Sb are not robust paleoredox proxies but examining their relative enrichment may be useful. These preliminary results indicate that a co-enrichment of both elements with Sb being more enriched than As could be the mark of the so-called particulate shuttle effect. Notably, Sb would be more sensitive to Mn-shuttling than As. If confirmed, this trend could be used to further identify the cause of As-enrichment in marine sediments impacted by cold seepage fluids.

Keywords: As / Sb / redox / cold seeps / particulate shuttle

Résumé – Enrichissements conjugués en arsenic et antimoine en dépôts marins, utilisés comme traceurs paléoenvironnementaux : résultats préliminaires. Deux métalloïdes sensibles à l'oxydoréduction, l'arsenic (As) et l'antimoine (Sb), sont examinés ici pour déterminer quelle peut être leur aide pour déchiffrer les conditions de dépôt du passé. Les facteurs d'enrichissement des deux éléments sont comparés pour un ensemble de formations géologiques et de dépôts marins couvrant une gamme relativement large de milieux paléo-environnementaux, allant des conditions oxiques aux conditions euxiniques. Ces travaux confirment que As et Sb ne sont pas des traceurs paléo-redox fiables, mais l'examen de leur enrichissement relatif peut être utile. Ces résultats préliminaires indiquent en effet qu'un co-enrichissement des deux éléments, tout en ayant Sb plus enrichi que As, pourrait être la marque de l'effet shuttle (transfert d'éléments chimiques par adsorption, de la colonne d'eau aux sédiments). Notamment, Sb serait plus sensible au transfert *via* les oxydes et (oxy)hydroxydes de Mn que ne l'est As. Si elle est confirmée, cette tendance pourrait être utilisée pour identifier plus aisément la cause de l'enrichissement en As dans les sédiments marins influencés par les suintements de fluides froids.

Mots clés : As / Sb / redox / suintements froids / transfert par adsorption

1 Introduction

Arsenic (As) and antimony (Sb) are two metalloids often mentioned together due to their belonging to group V of the periodic table, which gives them common characteristics (Tab. 1). They are most often mentioned for problems of toxicity and pollution of soils, lakes and drinking water supply; a large literature is available on this subject. On the other hand, relatively little work has been devoted to the conditions of accumulation of these two elements in marine sediments, when they are considered as paleo-environmental markers. Arsenic is much more studied than antimony in this regard. A recent study synthesized the complex geochemistry of sedimentary As (Tribovillard, 2020) and the behavior of this element in marine environments can be briefly summarized as follows. Arsenic is mainly brought to the sediments with (oxyhydr-) oxides of iron and manganese. If reducing conditions develop at or below the water-sediment interface, As can react with sulfide ions to form soluble species that can leave the sediment. On the other hand, As will remain trapped if it can react with iron sulfides (pyrite; see details in Tribovillard, 2020 and references therein). Arsenic and antimony show similarities and differences in the marine environment (Cutter, 1991; Cutter and Cutter, 1995, 2006; Cutter *et al.*, 2001; Chaillou *et al.*, 2008). Both are primarily transferred from the water column to the sediments by Fe and Mn (oxyhydr-)oxides (Qin *et al.*, 2019). However, they can have contrasting

*Corresponding author: nicolas.tribovillard@univ-lille.fr

Table 1. Basic values for the two key elements of this work.
Tableau 1. *Valeurs de base pour les deux éléments clés de ce travail.*

Elements	Electronic configuration	Mean oceanic concentration	Residence time in the ocean in years (1)	PAAS (2)	Upper Crust (3)	Aver. Shale (4)
As	[Ar] $3d^{1o}$ $4s^2$ $4p^3$	20 nmol/kg	39 000	1.5	4.8	13
Sb	[Kr] $4d^{1o}$ $5s^2$ $5p^3$	1.6 nmol/kg	5700	0.2	0.2	1.5
		(1) Broecker and Peng, 1982			*concentrations in ppm*	
		(2) Taylor and McLennan, 1985				
		(3) McLennan, 2001			(4) Wedepohl, 1995	

behaviors when subjected to variable redox conditions, depending on the amount of reactive iron available in the sediment (Chaillou *et al.*, 2008; Polack *et al.*, 2009; Ye *et al.*, 2020). Arsenic and Sb are readily incorporated into pyrite when it can form (Gregory *et al.*, 2015) but if trapping does not take place, it has been observed that As could be mobile under reducing conditions whereas Sb was preferably mobile under oxic conditions (Ye *et al.*, 2020 and references therein).

The goal of this study is to use the behavioral differences between these two metalloids to progress in paleoenvironmental reconstruction based on geochemical data. In a recent study (Tribovillard, 2020), a set of geological formations of very different age and depositional environment were examined to better understand how the enrichments in As could serve as a paleo-environmental proxy. The formations for which the data of Sb exist will be examined here and the relative enrichments in As and Sb will be compared. The differences and similarities between the distributions of these two elements will allow us to propose paleoenvironmental interpretations that can be transposed to many other marine deposits of the Phanerozoic.

2 Materials and methods

For the present work, the same geological formations as those examined in Tribovillard (2020) will be studied, except for the ones with no Sb data available. The formations are described in Tribovillard (2020) and references therein; the descriptions are summarized in Table 2. The analytical methods are also described in Tribovillard (2020). Some of the results are expressed through the enrichment factors of the elements. Enrichment factors (EF) were calculated as: X-EF = $[(X/Al)_{sample}/(X/Al)_{upper\ crust}]$, where X and Al represent the weight % concentrations of element X and Al, respectively. Samples were normalized using the average composition of the upper continental crust of the Earth (McLennan, 2001). The aluminum normalization is used to avoid the effects of variable dilution by carbonate and/or biogenic silica, although certain pitfalls may (seldom) accompany this approach when aluminum content is minimal as may be the case with carbonate rocks (see discussion in Van der Weijden, 2002 and Tribovillard *et al.*, 2006). Any value larger than 1.0 theoretically indicates the enrichment of an element relative to its average crustal abundance but, practically, an enrichment may be considered to be detectable when EF > 3 (Algeo and Tribovillard, 2009). Aluminum normalization and the calculation of enrichment factors have been retained in this paper because it is a convenient way to compare geological formations and sediments deposited in very different deposit contexts. However, this type of standardization is not always a panacea and the examination of elemental concentrations can also provide relevant information, especially when the chemical elements can be carried by particular mineralogical phases. By way of illustration, we can cite the work of Baux *et al.* (2019) who observed that glauconites carried relatively high concentrations of arsenic in the greenish sands of the Bay of Seine in Normandy.

3 Results

We will focus here upon the relationships between the respective enrichment factors in As and Sb, formation by formation. All the cross plots are illustrated with the Figure 1S available online (supplementary materials) and the results are summarized with Table 3. Four situations have been identified: situation 1 with low enrichments in both As and Sb, the other three situations with more or less pronounced enrichments in As and/or Sb. Situation 2 is when As is more enriched than Sb, situation 3 is when Sb is (slightly) more enriched than As, and situation 4 is when As and Sb enrichments are marked and proportional. Most of the time, the formations studied correspond to one situation only, but the samples of the Pigmy and Cariaco basins can be grouped in subsets belonging to two or three situations.

4 Interpretations

For the depositional environments subjected to oxic conditions (Jurassic Vaca Muerta, Argiles de Châtillon, Argiles de Wimereux, Cretaceous La Charce, Cenozoic Pigmy Basin prop parte), low enrichments in As and Sb are observed, with however enrichments in As a little more pronounced than those in Sb. This discrepancy may be related to a normalization bias. In the present work (as well as in Tribovillard, 2020), the enrichment factors are calculated using the upper crust composition of McLennan (2001), *i.e.*, 1.5 ppm for As and 0.2 ppm for Sb. This choice wad guided by the fact that the paper of McLennan (2001) is a widely-used reference in paleo-environmental reconstructions. The value for Sb is in the range of those reported by various authors (Hu and Gao, 2008, and references therein) but the As content is lower than that reported by Sims *et al.* (1990), Gao *et al.* (1998), Rudnick and

Table 2. Quick description of the main features of the geological formations or sedimentary deposits examined here with the key references for further information.
Tableau 2. *Description rapide des principales caractéristiques des formations géologiques ou des dépôts sédimentaires examinés ici avec les principales références pour plus d'informations.*

Formations/deposits	Descriptions	References
The Cariaco Basin, offshore Venezuela	This small-dimensioned basin yields several specific conditions: high, upwelling-stimulated, surface productivity, and restricted bottom waters prone to recurrent development of euxinic conditions. The organic-rich sediments of Pleistocene-Holocene age are also rich in diatoms and shows annual-type laminations.	Bout-Roumazeilles *et al.*, 2013; Riboulleau *et al.*, 2014
The Jurassic formations of the Boulonnais area (northern France)	Proximal lateral equivalent of the Kimmeridge Clay Fm., cropping alongshore the French coast of the English Channel. These sediments accumulated on a siliciclastic ramp subject to dominantly aerobic conditions with some episodes of dissolved oxygen restriction. The Kimmeridgian/Tithonian Argiles de Châtillon Fm. is made up with dark marls, mudstones and shales with marine-origin organic-matter. The Tithonian Bancs Jumeaux Fm. consists of dark marls, mudstones and siltstones with moderate marine-organic matter content. The paleoenvironments have been determined as suboxic. The Tithonian Argiles de Wimereux Fm. consists of dark marls, mudstones and siltstones with moderate to low organic-matter content. The paleoenvironments have been determined as normally oxygenated to suboxic. Cold seepage episodes were well recorded in the Bancs Jumeaux Fm.	Proust *et al.*, 1995; Deconinck *et al.*, 1996; Hatem *et al.*, 2014, 2016; Tribovillard *et al.*, 2015
The Vaca Muerta Formation, one of the most prolific source-rocks of the Neuquén Basin (Argentina)	This lithostratigraphic unit consists of dark shales, marls and limestones deposited during the Tithonian-Valanginian interval, as the result of a rapid and widespread marine transgression. In the southern part of the basin (Picún Leufú Anticline), the Vaca Muerta Fm. is interpreted as a prograding siliciclastic shelf with storm and turbidity flows, and with an episodic, moderate, limitation of marine circulation, at least during the beginning of the deposition. The Vaca Muerta Fm. did not record oxygen-limited conditions, contrary to the rest of the basin, except for the very base of the formation. In addition, the organic content of the rocks is rather poor.	Krim *et al.*, 2017, 2019
The "pseudo-biohermes" of Beauvoisin (S-E France)	The carbonate biohermes of Beauvoisin, in the Baronnies Mounts (Provence) developed at cold seep sites debouching at the basin bottom during the deposition of the Terres Noires Fm. Thick accumulation (2000 m) of monotonous, dark-colored, hemipelagic marls took place during the Bathonian to Oxfordian. The bioherms, rich in lucinids, developed on synsedimentary faults.	Gaillard *et al.*, 1985, 1992; Tribovillard *et al.*, 2013; Gay *et al.*, 2019
The Frasnian-Famennian boundary (late Devonian)	Formations encompassing the Frasnian–Famennian boundary (a major period of biodiversity crisis and environmental modifications). The formations were studied in France (La Serre and Coumiac sections, Montagne Noire), Morocco and Germany. The Upper Frasnian interval is commonly associated with the	Feist, 1985; Tribovillard *et al.*, 2004; Averbuch *et al.*, 2005; Riquier *et al.*, 2005, 2006, 2007, 2010

Table 2. (continued).

Formations/deposits	Descriptions	References
	deposition of one or two organic-rich units, the so-called Kellwasser (KW) horizons, deposited in outer shelf and epicontinental basin settings. Several factors controlling the KW organic-rich sediment accumulation have been proposed, and among them, enhanced productivity coupled to bottom-water oxygen-depletion. These factors have been connected to different driving mechanisms acting separately or combined, such as sea-level fluctuations, climatic variations, land plants spreading, volcanism or mountain building.	
The Gulf of Mexico	Sediments collected in the La Salle, Orca and Pigmy sub-basinson the northern border of the Gulf of Mexico (Louisiana continental slope). These sub-basins record both the terrigenous input from the North American continent and the tropical oceanic influences *via* the Loop Current. The sediments are dated of the Pleistocene and Holocene. The Orca Basin is an intra-slope depression that collects sedimentary particles of terrestrial origin (clastic and organic particles mainly supplied by the Mississippi River) and of marine origin (biogenic productivity). The basin is partly filled with dense brines leached from salt diapirs cropping out on the sea floor, and is permanently stratified. A strong pycnocline induces anoxic bottom conditions. The La Salle and Pigmy basins collect the same types of sedimentary particles but they are not stratified, and are thus not exposed to anoxic bottom conditions.	Tribovillard *et al.*, 2008; Montero-Serrano *et al.*, 2009, 2010, 2011
The Weddell Sea (ODP leg 113; 70°43.432'S, 13°49.195'W)	ODP Hole 692B was drilled in the eastern Weddell Sea on the shelf of the Dronning Maud Land. The site is located on the flank of a submarine canyon (Wegener Canyon), by 2875 m of water. Early Cretaceous black shales were cored and are described as Unit III, consisting of black to very dark grey claystone/ mudstone, with varying percentages of clay, carbonate, and organic matter. Parallel lamination is the dominant sedimentary structure; bioturbation is occasionally observed. The sediments are interpreted to have accumulated in an outer shelf/upper slope environment.	Barker *et al.*, 1988
Adélie Land region of East Antarctica	Piston core MD03-2603 was recovered at 3320 m depth, on the distal part of a mound located between the Cuvier and "D" canyons (Lat. 64°17.12 S, Long. 139°22.51 E), during the CADO cruise (Coring Adélie Diatom Oozes, MD130 Images X) on board R/V Marion DuFresne II. The sediment is composed of diatom ooze alternating with structureless greenish ooze and millimeter to centimeter thick green-to-dark seasonal laminations. Sediment lithology is very fine from clay to silt fraction.	Denis *et al.*, 2009; Presti *et al.*, 2011
La Charce Section	The La Charce Section (Vocontian Basin, SE France) shows typical pelagic alternations of burrowed, beige to light-grey limestone beds and medium-grey marls, deposited during the Hauterivian times, under the influence of Milankovitch-type climate variations. Benthic conditions were oxic to suboxic.	Baudin *et al.*, 1999; Van de Schootbrugge *et al.*, 2000, 2003

Table 3. Recapitulation of the distribution of the enrichment in As and Sb for the various formations or sediments studied here. Four situations have been distinguished, numbered 1 to 4. Two of them, namely, situations 2 and 3, are discussed as possible marks of Fe/Mn shuttling or cold-seep influences, respectively.

Tableau 3. *Récapitulation de la distribution des enrichissements en As et Sb pour les différentes formations ou sédiments étudiés ici. Quatre situations ont été distinguées, numérotées de 1 à 4. Deux d'entre elles, à savoir les situations 2 et 3, sont envisagées comme des signatures possibles d'influences de transfert par adsorption via les particules de Fe/Mn ou de suintements froids.*

Situation 1	Situation 2	Situation 3	Situation 4
low As, low Sb	As > Sb	Sb > As	As % SB
Orca Basin	Bancs Jumeaux Fm.	Cariaco Basin *pro parte*	Cariaco Basin *pro parte*
Pigmy Basin *pro parte*	Pigmy Basin *pro parte*	Pigmy Basin *pro parte*	Frasnian-Fammenian boundary, all sections but BO
E-Antarctica Adelie			
La Charce	Beauvoisin		
Argiles de Wimereux	Weddell Sea		
Argiles de Châtillon	Frasnian-Fammenian boundary, BO section		
Vaca Muerta Fm.	Vaca Muerta Fm. Sections COV, et VM1		
Sections 14/2, 12/7, 13/6, 14/1			

Gao (2003) and Hu and Gao (2008). As already pointed out to by Tribovillard (2020), the low As value of McLennan (2001) may artificially create an automatic > 1 value when calculating enrichment factors, thus erroneously suggesting some enrichment whereas such a bias does not occur using the consensual value of 0.2 ppm for Sb. Consequently, it is concluded here not to take into consideration the differences in the enrichment factors observed in the present work for formations deposited under oxic conditions. We may conclude that no significant enrichment in As and Sb are observed for sediments deposited under oxic conditions.

For reducing environments such as those studied here recording the Frasnian-Fammenian boundary, the respective enrichments in As and Sb are marked and largely proportional, except for the euxinic setting of La Serre (Montagne Noire, France) that yields scattered values. However, the sediments of the highly confined and anoxic Orca Basin (Gulf of Mexico) do not show significant enrichments in As and Sb. We have no explanation for this counter-intuition absence of enrichment despite reducing conditions: is it related to the over-salinity of the basin (Tribovillard *et al.*, 2008) or some basin reservoir effect (Algeo and Lyons, 2006) or the shortage of reactive iron and manganese (Tribovillard, 2020) or some other unsuspected factor? However, the idea to be retained is that sediments deposited under reducing conditions do not all show co-enrichments in As and Sb. This observation suggests that these metalloids are not robust redox proxies.

Still considering anoxic and/or euxinic depositional milieus, the Cariaco basin shows some enrichments in As and Sb. We observe similar distributions for both elements, with (1) gradually lower enrichments in As and Sb with increasing enrichment in molybdenum (Mo), that is, increasingly reducing conditions, and (2) a comparatively slightly higher enrichment in Sb relative to As when both elements are relatively enriched (Fig. 1). The Cariaco Basin yields a rather specific conjunction of factors:

- seasonal upwelling, stimulating a high productivity (Haug *et al.*, 1998);
- highly stratified water column prone to the development of euxinic conditions (Haug *et al.*, 1998; Aycard *et al.*, 2003; Quijada *et al.*, 2015, 2016);
- high sedimentation rates (Algeo and Lyons, 2006);
- active shuttling *via* Mn and Fe (oxy-hydr)oxides (Algeo and Tribovillard, 2009);
- relatively limited availability of reactive iron (Tribovillard, 2020).

The role of a high sedimentation rate can be discussed to account for the diminished enrichments in As and Sb when the basin was highly confined (*e.g.*, Crombez *et al.*, 2020; Liu and Algeo, 2020). Alternatively highly confined, hence reducing, conditions may have favored the formation of soluble As species, explaining why this element could be impoverished in the sediments (see discussion in Tribovillard, 2020, but this mechanism is less suitable for Sb). Lastly, the relative lack of reactive iron under highly reducing conditions may have limited the efficiency of As and Sb transfer from the water column to the sediment. The important point is that the Cariaco Basin is one of the rare situations where Sb is slightly more enriched than As. This is especially the case for samples showing relatively lower Mo enrichments, that is, regarding Cariaco, the samples for which the Mn/Fe shuttling was the highest.

This influence of the shuttle effect is even more visible in the case of the Pigmy Basin (Gulf of Mexico). Figure 2 shows the Pigmy samples in a diagram opposing the respective enrichments in U and Mo (Algeo and Tribovillard, 2009). The samples plotting in the area typical of the shuttle effect are also those with the highest Sb enrichment compared to As (Fig. 1). Thus, though our dataset regarding settings with a shuttle effect and available As & Sb data is quite limited, our

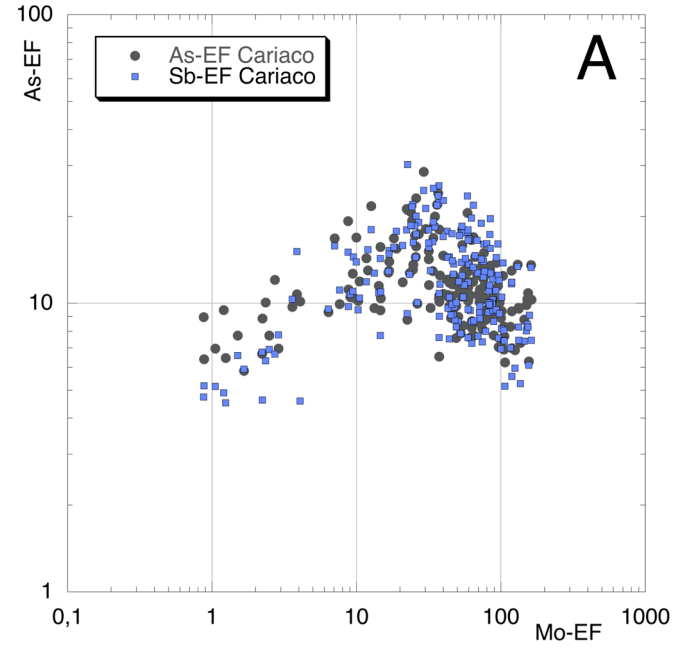

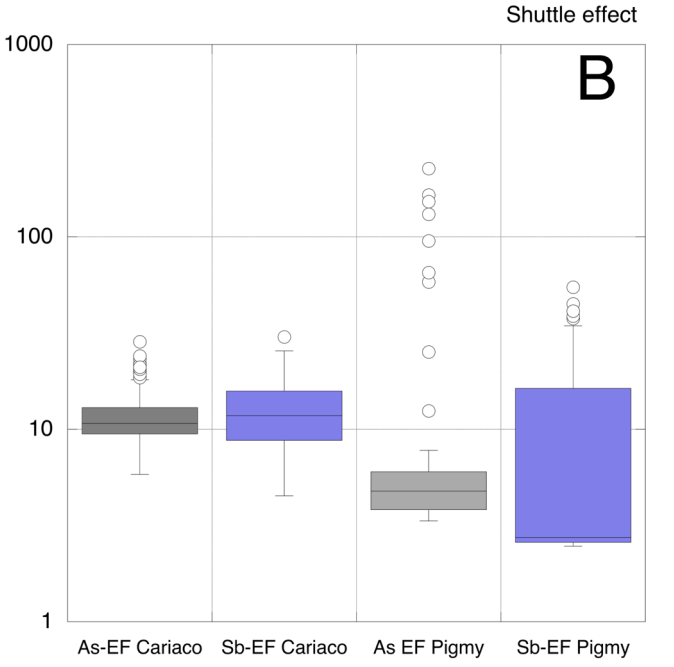

Fig. 1. A. Bivariate diagram opposing the enrichment factors of Mo (x-axis) to those of As and Sb (y-axis) for the Cariaco Basin samples. B. Box diagram showing the enrichment factors in As and Sb (As-EF and Sb-EF, respectively) for the sedimentary deposits influenced by the particulate shuttle effect.

Fig. 1. *A. Diagramme opposant les valeurs des facteurs d'enrichissement en Mo (abscisses) à celles desq facteurs d'enrichissement en As et Sb (ordonnées). B. Diagramme en « boîtes à moustaches » montrant les facteurs d'enrichissement en As et Sb (As-EF et Sb-EF, respectivement) pour les dépôts sédimentaires influencés par l'effet navette particulaire.*

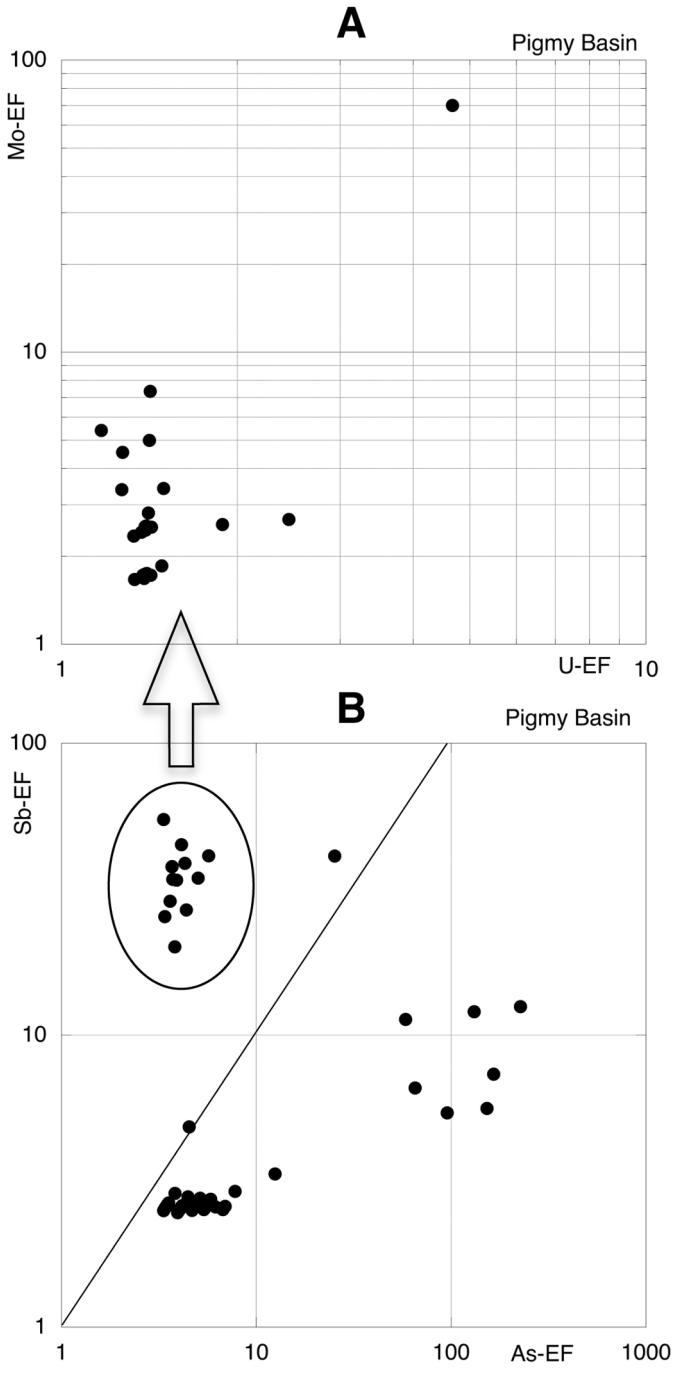

Fig. 2. A. Diagrams showing that the Pigmy Basin samples with Mo concentrations above the detection threshold value (A) yield low U enrichment factors (U-EF) but detectable Mo enrichments (Mo-EF), which indicates the influence of shuttling-mediated transfer of Mo to the sediment. B. The samples with detectable Mo concentrations are also those with high Sb enrichments (Sb-EF) relative to As values (As-EF).

Fig. 2. *A. Diagrammes montrant que les échantillons du Bassin de Pigmy avec des concentrations de Mo supérieures à la valeur du seuil de détection (A) montrent de faibles facteurs d'enrichissement en U (U-EF) mais des enrichissements détectables en Mo (Mo-EF), ce qui indique l'influence du transfert de Mo au sédiment, par des particules de Fe/Mn. B. Les échantillons avec des concentrations de Mo détectables sont également ceux avec des enrichissements élevés en Sb (Sb-EF) par rapport aux valeurs de As (As-EF).*

preliminary results strongly suggest that a higher Sb enrichment compared to As could be the mark of the Fe/Mn shuttling.

Qin *et al.* (2019) report that As and Sb are commonly captured by Fe and Mn (oxyhydr-)oxides but Sb is more reactive than As to the capture by Mn species. In addition, as reported by He and Hering (2009) and He *et al.* (2019), previous studies have reported the potential of manganese oxides (sensu lato, that, is, hydroxides and oxyhydroxides) in immobilizing the Sb present in water or sediments (Wang *et al.*, 2012; Basu *et al.*, 2014). Moreover, the capacity of Mn oxides for oxidizing and trapping Sb species has been demonstrated to be much higher than that of Fe oxyhydroxides (Thanabalasingam and Pickering, 1990; Belzile *et al.*, 2001; Wang *et al.*, 2012; He *et al.*, 2019). Lastly, As would be less sensitive to such a Mn-mediated capture, as indicated by the light enrichment in As observed on Mn species in Mediterranean sapropels (Robertson *et al.*, 2019; see He and Hering (2009) for a discussion about As solubilization/immobilization in presence of variable proportions of soluble Mn and Fe). Such a Mn-related transfer to the sediment may be hard to decipher after diagenesis because Mn is easily remobilized in sediments undergoing reducing conditions and released back to the water column. Iron may also be remobilized under reducing conditions but it is usually trapped within sediments in the form of insoluble iron sulfide or pyrite. Manganese is not so easily trapped: Mn carbonates and sulfides (rhodocrosite and alabandite, respectively) require specific conditions to be precipitated authigenically (Calvert and Pedersen, 1993; Tribovillard *et al.*, 2006). Therefore, Mn-mediated transfer of Sb and As may be carried out with no discernible Mn enrichment being recorded, but this shuttling could account for Sb being more enriched than As in some occurrences. If confirmed by further studies, this contrasted behavior of As and Sb could be a clue to detect past transfer of metalloids from seawater to sediment through Mn oxides (hydroxides and oxyhydroxides).

Enrichments in As and Sb are occasionally reported for sediments that underwent the influence of hydrothermal-fluid circulation or exhalation (plumes; Zeng *et al.*, 2018 and references therein); however, associations of these two elements have been seldom mentioned for sediments impacted by cold (hydrocarbon) seepage (Tribovillard *et al.*, 2013; Hu *et al.*, 2014; Chen *et al.*, 2016; Wang *et al.*, 2018, 2019a, 2019b; Zwicker *et al.*, 2018). Regarding cold seeps, most often, analyses are performed on associated authigenic minerals such as carbonates and/or sulfides, but only rarely on bulk sediments as is the case in the present study. Such authigenic substances may yield enrichments in Ba and Sr, as well as Ni, Co, Cu, Mo and W (Meyer-Dombard *et al.*, 2012; Wang *et al.*, 2019a) but these enrichments are not systematically observed (Liang *et al.*, 2017). Consequently, identifying the chemical signature of cold seepage is not straightforward for sediments that do not show obvious structures such as authigenic carbonate/sulfide chimneys, concretions or nodules. An additional pitfall is that authigenic carbonates may recrystallize during earliest diagenesis, which expels Mg and Sr and other trace elements from carbonates (Hatem *et al.*, 2014, 2016; Smrzka *et al.*, 2017) thus blurring the original imprint of cold seep fluids. Most often, unobtrusive influences of cold seepage may be deciphered using C, O and S stable isotope composition. Here, our observations show that the As-Sb covariations may be used as a diagnostic tool allowing for typifying cold seep signatures. Considering here the geological formations that undoubtedly underwent cold seepage influences, namely, the Bancs Jumeaux Fm. and the pseudo-bioherms of Beauvoisin, we observe no enrichment in Ba or Sr but the samples show enrichments in both As and Sb, with As-enrichment factors being larger than Sb-enrichment factors. The same is true for the cold seep-associated samples examined by Wang *et al.* (2019a). Lastly the same is also the case for samples of the VM1 section of the Vaca Muerta Fm., for which cold seepage influences have been suspected (Krim *et al.*, 2019). The geological objects concerned by hydrothermalism discussed here are in fact all linked to cold seeps. The limestone levels of the Boulonnais Tithonian Bancs Jumeaux Fm. and the Beauvoisin Oxfordian bioherms are linked to fluid circulations along synsedimentary faults. These fluids were rich in dissolved organic carbon (probably methane) and were at the origin of the development of particular faunas: oysters of small sizes (cm) almost exclusive in the Boulonnais, when faunas were associated there with cold seeps; Hatem *et al.* (2016), and dominant lucinids in the case of Beauvoisin bioherms. In the work of Wang *et al.* (2019a) on the Pliocene of the Chiahsien region (SW Taiwan), the objects of study were calcareous fluid conduits accompanied by lucinids. Finally, in the case of the VM1 section of the vaca Muerta formation, no evidence of fluid circulation was observed in the field (Krim *et al.*, 2017, 2019).

The enrichment in As of seepage-impacted sediments has already been reported and discussed at length by Tribovillard *et al.* (2013), Hu *et al.* (2014), Chen *et al.* (2016), Zwicker *et al.* (2018), Wang *et al.* (2018, 2019b). The debated point is to identify the driving force causing As enrichment: As-rich ascending fluids or reactive iron being released at seep sites and inducing a local shuttling, inducing in turn the capture and transfer of As? Here we complement the picture with Sb data and we observe that As is more enriched than Sb in the sediments of such environments (Fig. 3). From another standpoint, Bardelli *et al.* (2011) observed that bacterially-mediated carbonates can incorporate significant amounts of As (see also Smrzka *et al.*, 2019, 2020). In (past) cold seep settings, most of the authigenic carbonates result from bacterial processes, which could account for As being enriched more than Sb in the seep-related sediments examined here.

However, Table 3 and Figure 1S show that some depositional environments yield As enrichment relative to Sb but no discernible presence of past seep fluids (Weddell Sea, Vaca Muerta Covunco section, Pigmy Basin *pro parte*). We cannot be sure that no seepage occurred for these deposits but no evidences have ever been observed. Consequently, we cannot state unambiguously that seepage-impacted sediments always show As and Sb enrichments with As being more enriched than Sb. Nevertheless, our results suggest that a shuttle-mediated enrichment would favor Sb over As (especially if the shuttling is mediated by Mn and not Fe alone), whereas the opposite is observed here for the sites of ascertained seepage influences. Therefore, it is suggested that shuttling was not the driving force accounted for As and Sb enrichments at Beauvoisin (pseudo-bioherms) or in the Boulonnais (Bancs Jumeaux Fm.).

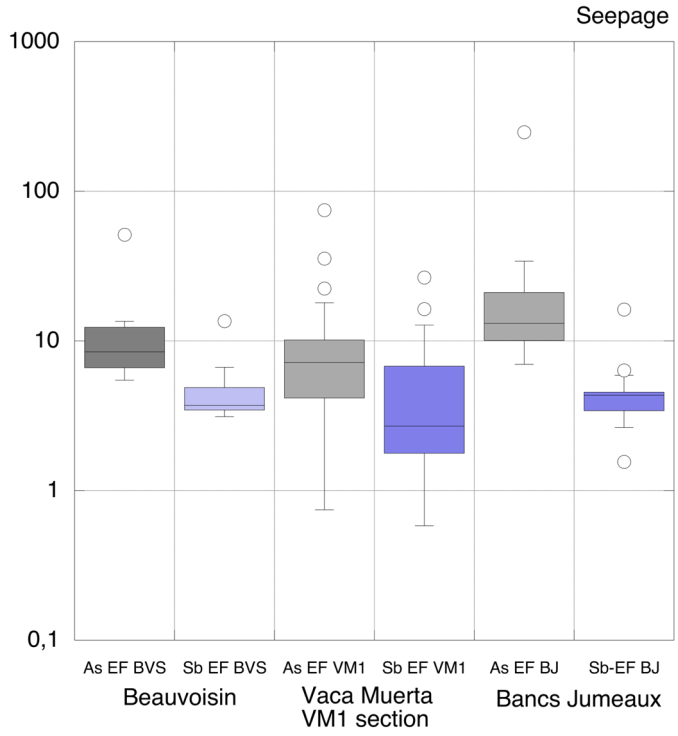

Fig. 3. Box diagram showing the enrichment factors in As and Sb (As-EF and Sb-EF, respectively) for the sedimentary deposits influenced by cold-seep fluids. In such box plots, each box encloses 50% of the data with the median value of the variable displayed as a line. The top and bottom of the box mark the limits of ± 25% of the variable population. The lines extending from the top and bottom of each box mark the minimum and maximum values within the data set that fall within an acceptable range. Any value outside of this range, called an outlier, is displayed as an individual point.

Fig. 3. *Diagramme en « boîtes à moustaches » montrant les facteurs d'enrichissement en As et Sb (As-EF et Sb-EF, respectivement) pour les dépôts sédimentaires influencés par les fluides de suintement froids. Dans ces « boîtes à moustaches », chaque boîte englobe 50 % des données avec la valeur médiane de la variable affichée sous forme de ligne. Le sommet et la base de la case indiquent les limites de ± 25 % de la population variable. Les lignes qui partent du haut et du bas de chaque case indiquent les valeurs minimales et maximales de l'ensemble de données qui se situent dans une plage acceptable. Toute valeur en dehors de cette plage, appelée valeur aberrante, est affichée en tant que point individuel.*

5 Conclusion

A recent synthesis illustrated that As cannot be looked at as a simple-to-use redox proxy (Tribovillard, 2020). The present work further shows that the combination of As and Sb cannot reliably help to reconstruct paleoredox situations, although these metalloids are redox-sensitive elements. However, our results indicate that As and Sb enrichments may be used to discuss two paleoenvironmental situations in the sedimentary record: cold seep-impacted sediments and settings prone to the particulate shuttle process. For these two types of situations, an enrichment is As is observed; however, disentangling the very cause of metal(loid) enrichment in the case of cold seepage is not easy: direct enrichment by ascending fluids or shuttling induced by the seep panache (Tribovillard, 2020 and discussion therein)? To be further assessed, the preliminary results presented here need to be tested in a larger number of cases. Nevertheless, our work suggests that coeval, marked enrichments in As and Sb with Sb being (slightly) more enriched than As, could be a signature of Fe/Mn shuttling. If true, on the basis of the situations studied here, the metalloid enrichments observed at some seep sites would result from direct enrichment by seeping fluids rather than from seepage-released iron and/or manganese, shuttling around seep sites.

Supplementary Material

Fig. 1S. Bivariate diagram illustrating the relationships between the enrichment factors of As and Sb for the Devonian sections yielding the samples of the Kellwasser horizons (A), all the samples but the La Serre section (B), the samples of the La Serre section (C), the Cariaco Basin (D), the Jurassic bioconstructions of the Terres Noires Fm. (SE-France) (E), the Orca and Pigmy basins of the Gulf of Mexico (F), the various sections of the Vaca Muerta Fm. of Argentina (G), the marl formations of the Boulonnais area (N-France; AW stands for Argiles de Wimereux, BJ stands for Bancs Jumeaux and ADC stands for Argiles de Châtillon) (H), the Weddell Sea (I) and the Hauterivian La Charce section (J).

Diagramme croisé illustrant les relations entre les facteurs d'enrichissement de As et Sb pour les coupes dévoniennes montrant les échantillons des horizons Kellwasser (A), tous les échantillons sauf ceux de la coupe de La Serre (B), les échantillons de la coupe de La Serre (C), le Bassin de Cariaco (D), les bioconstructions jurassiques des Terres Noires (SE-France) (E), les bassins Orca et Pigmy du golfe du Mexique (F), les différentes sections de la Vaca Muerta d'Argentine (G), les formations marneuses du Boulonnais (N-France; AW signifie Argiles de Wimereux, BJ signifie Bancs Jumeaux et ADC signifie Argiles de Châtillon) (H), la mer de Weddell (I) et l'Hauterivien de la coupe de La Charce (J).

The Supplementary Material is available at http://www.bsgf/10.1051/bsgf/2021034/olm.

Acknowledgement. Thanks a lot to all those who shared their data with me. I am grateful to Anne Murat (CNAM-Intechmer at Cherbourg) and an anonymous reviewer for their helpful suggestions that opened perspectives. Thanks to the editors of the journal, Cécile Robin (Université Rennes 1) and Laurent Jolivet (Sorbonne Université, Paris).

References

Algeo TJ, Lyons TW. 2006. Mo-total organic carbon covariation in modern anoxic marine environments: Implications for analysis of paleoredox and paleohydrographic conditions. *Paleoceanography* 21: PA1016. https://doi.org/10.1029/2004PA001112.

Algeo TJ, Tribovillard N. 2009. Environmental analysis of paleoceanographic systems based on molybdenum-uranium co-variation. *Chemical Geology* 268: 211–225.

Averbuch O, Tribovillard N, Devleeschouwer X, Riquier L, Mistiaen B, Van Vliet-Lanoe B. 2005. Mountain building-enhanced continental weathering and organic carbon burial as major causes for climatic cooling at the Frasnian-Famennian boundary (ca. 376 Ma BP). *Terra Nova* 17: 33–42.

Aycard M, Derenne S, Largeau C, Tribovillard N, Baudin F. 2003. Formation pathways of proto-kerogens in Holocene sediments of the upwelling influenced Cariaco Trench, Venezuela. *Organic Geochemistry* 34: 701–718.

Bardelli F, Benvenuti M, Costagiola P, Di Benedetto F, Lattanzi P, Meneghini C, *et al.* 2011. Arsenic uptake by natural calcite: An XAS study. *Geochimica et Cosmochimica Acta* 75: 3011–3023.

Barker PE, Kennett JP, *et al.* 1988. Proc. ODP, Init. Repts, 113: College Station, TX (Ocean Drilling Program). https://doi.org/10.2973/odp.proc.ir.113.1988.

Basu A, Saha D, Saha R, Ghosh T, Saha B. 2014. A review on sources, toxicity and remediation technologies for removing arsenic from drinking water. *Res. Chem. Interm.* 40: 447–485.

Baudin F, Bulot LG, Cecca F, Coccioni R, Gardin S, Renard M. 1999. Un équivalent du « Niveau Faraoni » dans le Bassin du Sud-Est de la France, indice possible d'un événement anoxique fini-hauterivien étendu à la Téthys méditerranéenne. *Bulletin de la Société géologique de France* 170: 487–498.

Baux N, Murat A, Faivre Q, Lesourd S, Poizot E, Méar Y, *et al.* 2019. Sediment dynamic equilibrium, a key for assessing a coastal anthropogenic disturbance using geochemical tracers: Application to the eastern part of the Bay of Seine. *Continental Shelf Research* 175: 87–98.

Belzile N, Chen YW, Wang ZJ. 2001. Oxidation of antimony(III) by amorphous iron and manganese oxyhydroxides. *Chem. Geol.* 174: 379–387.

Bout-Roumazeilles V, Riboulleau A, Armynot du Châtelet E, Lorenzoni L, Tribovillard N, Murray RW, *et al.* 2013. Clay mineralogy of surface sediments as a tool for deciphering river contributions to the Cariaco Basin (Venezuela). *Journal of Geophysical Research – Oceans* 118: 750–761.

Broecker WS, Peng T-H. 1982. Tracers in the Sea. Palisades, NY, Columbia University. Eldigio Press, 689 p.

Calvert SE, Pedersen TF. 1993. Geochemistry of recent oxic and anoxic sediments: Implications for the geological record. *Marine Geology* 113: 67–88.

Chaillou G, Schäfer J, Blanc G, Anschutz P. 2008. Mobility of Mo, U, As, and Sb within modern turbidites. *Marine Geology* 254: 171–179.

Chen F, Hu Y, Feng D, Zhang X, Cheng S, Cao J, *et al.* 2016. Evidence of intense methane seepages from molybdenum enrichments in gas hydrate-bearing sediments of the northern South China Sea. *Chemical Geology* 443: 173–181.

Crombez V, Rohais S, Euzen T, Riquier L, Baudin F, Hernandez-Bilbao E. 2020. Trace metal elements as paleoenvironmental proxies: Why should we account for sedimentation rate variations? *Geology* 48: 839–843.

Cutter GA. 1991. Dissolved arsenic and antimony in the Black Sea. *Deep Sea Res.* Part A 38(suppl): S825–S843.

Cutter GA, Cutter LS. 1995. Behavior of dissolved antimony, arsenic, and selenium in the Atlantic Ocean. *Mar. Chem.* 49: 295–306.

Cutter GA, Cutter LS. 2006. Biogeochemistry of arsenic and antimony in the North Pacific Ocean. *Geochemistry Geophysics Geosystems* 7: Q05M08.

Cutter GA, Cutter LS, Featherstone AM, Lohrenz SE. 2001. Antimony and arsenic biogeochemistry in the western Atlantic Ocean. *Deep Sea Res* Part II 48: 2895–2915.

Deconinck J-F, Geyssant JR, Proust J-N, Vidier JP. 1996. Sédimentologie et biostratigraphie des dépôts kimméridgiens et tithoniens du Boulonnais. *Annales de la Société Géologique du Nord* 4: 157–170.

Denis D, Crosta X, Schmidt S, Carson DS, Ganeshram RS, Renssen H, *et al.* 2009, Holocene glacier and deep water dynamics, Adélie Land region, East Antarctica. *Quaternary Science Reviews* 28: 1291–1303.

Feist R. 1985. Devonian stratigraphy of the South-eastern Montagne Noire (France). *Cour. Forsch Inst. Senckenberg* 75: 331–352.

Gao S, Luo TC, Zhang BR, Zhang HF, Han YW, Zhao ZD, *et al.* 1998. Chemical composition of the continental crust as revealed by studies in East China. *Geochimica et Cosmochimica Acta* 62: 1959–1975.

Gaillard C, Bourseau JP, Boudeulle M, Pailleret P, Rio M, Roux M. 1985. Les pseudobiohermes de Beauvoisin (Drôme) : un site hydrothermal sur la marge téthysienne l'Oxfordien ? *Bulletin de la Société Géologique de France Série* 8: 69–78.

Gaillard C, Rio M, Rolin Y. 1992. Fossil chemosynthetic communities related to vents or seeps in sedimentary basins: The pseudobiohermes of south-eastern France compared to other world examples. *Palaios* 7: 451–465.

Gay A, Lopez M, Potdevin J-L, Vidal V, Varas G, Favier A, *et al.* 2019. 3D morphology and timing of the giant fossil pockmark of Beauvoisin, SE Basin of France. *Journal of the Geological Society* 176: 61–77.

Gregory DD, Large RR, Halpin JA, Baturina EL, Lyons TW, Wu S, *et al.* 2015. Trace element content in sedimentary pyrite in black shales. *Economic Geology* 110: 1389–1410.

Hatem E, Tribovillard N, Averbuch O, Vidier D, Sansjofre P, Birgel D, *et al.* 2014. Oyster patch reefs as indicators of fossil hydrocarbon seeps induced by synsedimentary faults. *Marine and Petroleum Geology* 55: 176–185.

Hatem E, Tribovillard N, Averbuch O, Sansjofre P, Adatte T, Guillot F, *et al.* 2016. Early diagenetic formation of carbonates in a clastic-dominated ramp environment impacted by synsedimentary faulting-induced fluid seepage – Evidence from the Late Jurassic Boulonnais Basin (N France). *Marine and Petroleum Geology* 72C: 12–29.

Haug GH, Pedersen TF, Sigman DM, Calvert SE, Nielsen B, Peterson LC. 1998. Glacial/interglacial variations in production and nitrogen fixation in the Cariaco Basin during the last 580 kyr. *Paleoceanogry* 13: 427–432.

He M, Wang N, Long X, Zhang C, Ma C, Zhong Q, *et al.* 2019. Antimony speciation in the environment: Recent advances in understanding the biogeochemical processes and ecological effects. *J. Environ. Sci.* 75: 14–39.

He YT, Hering JG. 2009. Enhancement of arsenic(III) sequestration by manganese oxides in the presence of iron(II). *Water Air and Soil Pollution* 203: 359–362.

Hu Z, Gao S. 2008. Upper crustal abundances of trace elements: A revision and update. *Chemical Geology* 253: 205–221.

Hu Y, Feng D, Peckmann J, Roberts HH, Chen D. 2014. New insights into cerium anomalies and mechanisms of trace metal enrichment in authigenic carbonate from hydrocarbon seeps. *Chemical Geology* 381: 55–66.

Krim N, Bonnel C, Aubourg C, Imbert P, Tribovillard N. 2017. Paleoenvironmental evolution of the southern Neuquén Basin (Argentina) during the Tithonian-Berrisian interval (Vaca Muerta and Picun Leufu formations): A multi-proxy approach. *Bulletin Société Géologique de France* 188: 34. https://doi.org/10.1051/bsgf/2017196.

Krim N, Tribovillard N, Riboulleau A, Bout-Roumazeilles V, Bonnel C, Imbert P, *et al.* 2019. Reconstruction of paleoenvironmental conditions of the Vaca Muerta Formation in the southern part of the Neuquén Basin, using clay-mineral assemblages, inorganic geochemistry and Rock Eval data. *Marine and Petroleum Geology* 103: 176–201.

Liang Q, Hu Y, Feng D, Peckmann J, Chen L, Yang S, *et al.* 2017. Authigenic carbonates from newly discovered active cold seeps on the northwestern slope of the South China Sea: Constraints on fluid sources, formation environments, and seepage dynamics. *Deep Sea Research* Part I 124: 31–41.

Liu J, Algeo TJ. 2020. Beyond redox: Control of trace-metal enrichment in anoxic marine facies by watermass chemistry and sedimentation rate. *Geochimica et Cosmochimica Acta* 287: 296–317.

McLennan SM. 2001. Relationships between the trace element composition of sedimentary rocks and upper continental crust. *Geochemistry, Geophysics, Geosystems* 2: 2000GC000109.

Meyer-Dombard DR, Price RE, Pichler T, Amend JP. 2012. Prokaryotic populations in arsenic-rich shallow-sea hydrothermal sediments of Ambitle Island, Papua New Guinea. *Geomicrobiology Journal* 29: 1–17.

Montero-Serrano JC, Bout-Roumazeilles V, Tribovillard N, Sionneau T, Riboulleau A, Bory A, *et al.* 2009. Sedimentary evidence of deglacial megafloods in the northern Gulf of Mexico (Pigmy Basin). *Quaternary Science Reviews* 28: 3333–3347.

Montero-Serrano JC, Martinez M, Riboulleau A, Tribovillard N, Márquez G, Gutiérrez-Martín JV. 2010. Assessment of the oil source-rock potential of the Pedregoso Formation (Early Miocene) in the Falcón Basin of Northwestern Venezuela. *Marine and Petroleum Geology* 27(5): 1107–1118.

Montero-Serrano J-C, Bout-Roumazeilles V, Carlson AE, Tribovillard N, Bory A, Meunier G, *et al.* 2011. Contrasting rainfall patterns over North America during the Holocene and last interglacial as recorded by sediments of the northern Gulf of Mexico. *Geophysical Research Letters* 38: L14709. https://doi.org/10.1029/2011GL048194.

Polack R, Chen Y-W, Belzile N. 2009. Behaviour of Sb(V) in the presence of dissolved sulfide under controlled anoxic aqueous conditions. *Chemical Geology* 262: 179–185.

Presti M, Barbara L, Denis D, Schmidt S, De Santis L, Crosta X. 2011. Sediment delivery and depositional patterns off Adélie Land (East Antarctica) in relation to late Quaternary climatic cycles. *Marine Geology* 284: 96–113.

Proust J-N, Deconinck J-F, Geyssant JR, Herbin J-P, Vidier JP. 1995. Sequence analytical approach to the Upper Kimmeridgian-Lower Tithonian storm-dominated ramp deposits of the Boulonnais (Northern France). A landward time-equivalent to offshore marine source rocks. *Geol. Rundsch.* 84: 255–271.

Qin HB, Uesugi S, Yang S, Tanaka M, Kashiwabara T, Itai T, *et al.* 2019. Enrichment mechanisms of antimony and arsenic in marine ferromanganese oxides: Insights from the structural similarity. *Geochimica et Cosmochimica Acta*, in press.

Quijada M, Riboulleau A, Monnet C, Tribovillard N. 2015. Neutral aldoses derived from sequential acid hydrolysis of sediments as indicators of diagenesis over 120 000 years. *Organic Geochemistry* 81: 53–63.

Quijada M, Riboulleau A, Faure P, Michels R, Tribovillard N. 2016. Organic matter sulfurization on protracted diagenetic timescales: The possible role of anaerobic oxidation of methane. *Marine Geology* 381: 54–66.

Riboulleau A, Bout-Roumazeilles V, Tribovillard N. 2014. Controls on detrital sedimentation in the Cariaco Basin during the last climatic cycle: Insight from clay minerals. *Quaternary Science Reviews* 94: 62–73.

Riquier L, Tribovillard N, Averbuch O, Joachimski MM, Racki G, Devleeschouwer X, *et al.* 2005. Productivity and bottom water redox conditions at the Frasnian-Famennian boundary on both sides of the Eovariscan Belt: Constraints from trace-element geochemistry. In: Over DJ, Morrow JR, Wignall PB, eds. *Understanding Late Devonian and Permian-Triassic Biotic and Climatic Events: Towards an Integrated Approach*. Developments in Palaeontology and Stratigraphy, vol. 20, Elsevier, pp. 199–224.

Riquier L, Tribovillard N, Averbuch O, Devleeschouwer X, Riboulleau A. 2006. The Late Frasnian Kellwasser horizons of the Harz Mountains (Germany): Two oxygen-deficient periods resulting from different mechanisms. *Chem. Geol.* 233: 137–155.

Riquier L, Averbuch O, Tribovillard N, El Albani A, Lazreq N, Chakiri S. 2007. Environmental changes at the Frasnian-Famennian boundary in Central Morocco (Northern Gondwana): Integrated rock-magnetic and geochemical studies. In: Becker T, Kirchgasser B, eds. *Devonian Events and Correlations*. Geological Society, London, Special Publications, 278, pp. 197–217.

Riquier L, Averbuch O, Devleeschouwer X, Tribovillard N. 2010. Diagenetic versus detrital origin of the magnetic susceptibility variations in some carbonate Frasnian-Famennian boundary sections from Northern Africa and Western Europe: Implications for paleoenvironmental reconstructions. *International Journal of Earth Sciences* 99: S57–S73. https://doi.org/10.1007/s00531-009-0492-7.

Robertson AHF, Necdet M, Raffi I, Chen G. 2019. Early Messinian manganese deposition in NE Cyprus related to cyclical redox changes in a silled hemipelagic basin prior to the Mediterranean salinity Crisis. *Sediment. Geol.* 385: 126–148.

Rudnick R, Gao S. 2003. Composition of the continental crust. In: Rudnick RL, ed. *The crust*. In: Holland HD, Turekian KK, eds. *Treatise on Geochemistry*, vol. 3. Oxford: Elsevier–Pergamon, pp. 1–64.

Sims KWW, Newsom HE, Gladneys ES. 1990. Chemical fractionation during formation of the Earth's core and continental crust: Clues from As, Sb, W and Mo. In: Newsome HF, Jones JH, eds. *Origin of the Earth*. Oxford University Press, pp. 291–317.

Smrzka D, Zwicker J, Kolonic SF, Birgel D, Little CTS, Marzouk AM. 2017. Methane seepage in a Cretaceous greenhouse world recorded by an unusual carbonate deposit from the Tarfaya Basin, Morocco. *The Depositional Record*. https://doi.org/10.1002/dep2.24.

Smrzka D, Zwicker J, Bach W, Feng D, Himmler T, Chen D, *et al.* 2019. The behavior of trace elements in seawater, sedimentary pore water, and their incorporation into carbonate minerals: A review. *Facies* 65: 41. https://doi.org/10.1007/s10347-019-0581-4.

Smrzka D, Feng D, Himmler T, Zwicker J, Hu Y, Monien P, *et al.* 2020. Trace elements in methane-seep carbonates: Potentials, limitations, and perspectives. *Earth-Science Reviews* 208: 103263.

Taylor SR, McLennan SM. 1985. The continental crust: Its composition and evolution. Oxford: Blackwell, 312 p.

Thanabalasingam P, Pickering WF. 1990. Specific sorption of antimony(III) by the hydrous oxides of Mn, Fe, and Al. *Water Air Soil Pollut.* 49: 175–185.

Tribovillard N. 2020. Arsenic in marine sediments: how robust a redox proxy? *Palaeogeography, Palaeoclimatology, Palaeoecology* 550: 109745.

Tribovillard N, Averbuch O, Devleeschouwer X, Racki G, Riboulleau A. 2004. Deep-water anoxia over the Frasnian-Famennian boundary (La Serre, France): A tectonically-induced oceanic anoxic event? *Terra Nova* 16(5): 288–295.

Tribovillard N, Algeo TJ, Lyons TW, Riboulleau A. 2006. Trace metals as paleoredox and paleoproduc-tivity proxies: An update. *Chem. Geol.* 232: 12–32.

Tribovillard N, Bout-Roumazeilles V, Algeo TJ, Lyons TW, Sionneau T, Montero-Serrano JC, *et al.* 2008. Paleodepositional conditions in the Orca Basin as inferred from organic matter and trace metal contents. *Marine Geology* 254: 62–72.

Tribovillard N, Armynot du Châtelet E, Gay A, Barbecot F, Sansjofre P, Potdevin J-L. 2013. Geochemistry of cold seepage-impacted sediments: Per-ascensum or per-descensum trace metal enrichment? *Chemical Geology* 340: 1–12.

Tribovillard N, Hatem E, Averbuch O, Barbecot F, Bout-Roumazeilles V, Trentesaux A. 2015. Iron availability as a dominant control on the primary composition and diagenetic overprint of organic-matter-rich rocks. *Chemical Geology* 401: 67–82.

Van de Schootbrugge B, Föllmi KB, Bulot LG, Burns SJ. 2000. Paleoceanographic changes during the early Cretaceous (Valanginian Hauterivian): Evidence from oxygen and carbon stable isotopes. *Earth and Planetary Science Letters* 181: 15–31.

Van de Schootbrugge B, Kuhn O, Adatte T, Steinmann P, Föllmi K. 2003. Decoupling of P- and Corg-burial following Early Cretaceous (Valanginian–Hauterivian) platform drowning along the NW Tethyan margin. *Palaeogeography, Palaeoclimatology, Palaeoecology* 199: 315–331.

Van der Weijden CH. 2002. Pitfalls of normalization of marine geochemical data using a common divisor. *Marine Geology* 184: 167–187.

Wang X, Li N, Feng D, Hu Y, Bayon G, Liang Q, *et al.* 2018. Using chemical compositions of sediments to constrain methane seepage dynamics: A case study from Haima cold seeps of the South China Sea. *Journal of Asian Earth Sciences* 168: 137–144.

Wang Q, Chen D, Peckmann J. 2019a. Iron shuttle control on molybdenum, arsenic and antimony enrichment in Pliocene methane-seep carbonates from the southern Western Foothills, Southwestern Taiwan. *Marine and Petroleum Geology* 100: 263–269.

Wang X, Bayon G, Kim JH, Lee D-H, Kim D, Guéguen B, *et al.* 2019b. Trace element systematics in cold seep carbonates and associated lipid compounds. *Chemical Geology* 528: 119277.

Wang X, He M, Lin C, Gao Y, Zheng L. 2012. Antimony(III) oxidation and antimony(V) adsorption reactions on synthetic manganite. *Chem. Erde-Geochem.* 72: 41–47.

Wedepohl KH. 1995. The composition of the continental crust. *Geochimica et Cosmochimica Acta* 59: 1217–1232.

Ye L, Meng X, Jing C. 2020. Influence of sulfur on the mobility of arsenic and antimony during oxic-anoxic cycles: differences and competition. *Geochimica et Cosmochimica Acta* 288: 51–67.

Zeng Z, Wang X, Chen C-TA, Qi H. 2018. Understanding the compositional variability of the major components of hydrothermal plumes in the Okinawa Trough. *Geofluids*, Article ID 1536352. https://doi.org/10.1155/2018/1536352.

Zwicker J, Smrzka D, Himmler T, Monien P, Gier S, Goedert JL, *et al.* 2018. Rare earth elements as tracers for microbial activity and early diagenesis: A new perspective from carbonate cements of ancient methane-seep deposits. *Chemical Geology* 501: 77–85.

Cite this article as: Tribovillard N. 2021. Conjugated enrichments in arsenic and antimony in marine deposits used as paleoenvironmental proxies: preliminary results, *BSGF - Earth Sciences Bulletin* 192: 39.